Biosensors and Bioelectronics 70 (2015) 130–136

Contents lists available at ScienceDirect

Biosensors and Bioelectronics

journal homepage: www.elsevier.com/locate/bios

An electrochemical DNA biosensor for evaluating the effect of mix anion in cellular fluid on the antioxidant activity of CeO_2 nanoparticles

Yanwu Zhai [b], Yan Zhang [a], Fei Qin [a], Xin Yao [a,*]

[a] School of Chemistry and Chemical Engineering, University of Chinese Academy of Sciences, Beijing 100049, PR China
[b] College of Materials Science and Opto-Electronic Technology, University of Chinese Academy of Sciences, Beijing 100049, PR China

ARTICLE INFO

Article history:
Received 8 December 2014
Received in revised form
12 March 2015
Accepted 13 March 2015
Available online 14 March 2015

Keywords:
CeO_2 nanoparticles
DNA electrochemical biosensor
Anion affection
Antioxidant activity

ABSTRACT

CeO_2 nanoparticles are of particular interest as a novel antioxidant for scavenging free radicals. However, some studies showed that they could cause cell damage or death by generating reactive oxygen species (ROS). Up to now, it is not well understood about these paradoxical phenomena. Therefore, many attentions have been paid to the factors that could affect the antioxidant activity of CeO_2 nanoparticles. CeO_2 nanoparticles would inevitably encounter body fluid environment for its potential medical application. In this work the antioxidant activity behavior of CeO_2 nanoparticles is studied in simulated cellular fluid, which contains main body anions (HPO_4^{2-}, HCO_3^-, Cl^- and SO_4^{2-}), by a method of electrochemical DNA biosensor. We found that in the solution of Cl^- and SO_4^{2-}, CeO_2 nanoparticles can protect DNA from damage by hydroxyl radicals, while in the presence of HPO_4^{2-} and HCO_3^-, CeO_2 nanoparticles lose the antioxidant activity. This can be explained by the cerium phosphate and cerium carbonate formed on the surface of the nanoparticles, which interfere with the redox cycling between Ce^{3+} and Ce^{4+}. These results not only add basic knowledge to the antioxidant activity of CeO_2 nanoparticles under different situations, but also pave the way for practical applications of nanoceria. Moreover, it also shows electrochemical DNA biosensor is an effective method to explore the antioxidant activity of CeO_2 nanoparticles.

1. Introduction

Recently, CeO_2 nanoparticles as an excellent antioxidant have drawn more and more attentions because of their application in medicine. It was found that CeO_2 nanoparticles can protect selectively cultured normal mammary epithelial cells after irradiation, whereas have no positive effect on the tumor counterparts (MCF7 cells) treated under identical conditions (Tarnuzzer et al., 2005). CeO_2 nanoparticles are also reported to play a role in neuroprotection (Heckman et al., 2013; Schubert et al., 2006; Yu et al., 2009), antiinflammation (Arya et al., 2013; Bakht et al., 2013; Hirst et al., 2009), cardioprotection (Niu et al., 2007; Pagliari et al., 2012) and retinaprotection (McGinnis et al., 1999; Rich et al., 2000) in cells. However, other studies indicated that CeO_2 nanoparticles have biotoxicity by causing a series of adverse response through oxidative stress (Auffan et al., 2009). It was reported that, nanoceria induced intracellular ROS and ROS dependent signals in human bronchial epithelial cells (Beas2B) (Park et al., 2008). Inhaled cerium oxide nanoparticles were also believed to induce an inflammatory in CD1 mice, resulting in necrosis, proteinosis, fibrosis and granulomas in the pulmonary tissue and tubular degeneration giving rise to coagulative necrosis in kidneys (Aalapati et al., 2014). Based on these paradoxical phenomena many works have been done to study the factor that could affect the antioxidant activity of CeO_2 nanoparticles, which could also help to understand the mechanism of antioxidant activity of CeO_2 nanoparticles. The significant difference on the surface chemistry of nanoceria and reaction media in relevant reports may account for the paradoxical phenomena (Celardo et al., 2011; Karakoti et al., 2010). To some extent, nanoceria with proper surface chemistry can be obtained through controlling the processor and experiment parameter (Chen et al., 2006; Korsvik et al., 2007; Niu et al., 2007; Xue et al., 2011). It is found the concentration and size of CeO_2 nanoparticles could affect the antioxidant activity to some extent (Lee et al., 2013; Tsai et al., 2007; Xue et al., 2011). Recently, we found the exposed crystal planes of CeO_2 nanoparticles could also affect its antioxidant activity (Zhang et al., 2014). However, all those factors affected the antioxidant activity of CeO_2 nanoparticles in a limited degree, and they were not the key factor for the loss of antioxidant activity of CeO_2 nanoparticles. It was found that the antioxidant activity of the nanoparticles was susceptible to external anions, and the influences depended on the anion type

* Corresponding author. Fax: +86 10 88256092.
E-mail address: yaox@ucas.ac.cn (X. Yao).

http://dx.doi.org/10.1016/j.bios.2015.03.030
0956-5663/

(Singh et al., 2011; Xue et al., 2012). PO_4^{3-} could make CeO_2 nanoparticles lose antioxidant activity by forming cerium phosphate on the particles' surface. However, as mentioned before, CeO_2 nanoparticles showed antioxidant effect in kinds of cells. In view of many other molecules existing in cells, whether the anion ions in body fluid could still interact with CeO_2 nanoparticles should be considered (Singh et al., 2011). But up to now, no work has been done on whether CeO_2 nanoparticles still possess the antioxidant activity in body fluid environment.

Most research systems on the antioxidant activity of CeO_2 nanoparticles are based on different kinds of cell systems, which are complicate and hard to control all the factors. In this report, the simulated intracellular fluid and intercellular fluid were prepared, which consisted of main anion HPO_4^{2-}, HCO_3^-, Cl^- and SO_4^{2-} with corresponding concentration in vivo. Then, the behavior of CeO_2 nanoparticles in different simulated cellular fluid was studied through a method of electrochemical DNA biosensor, the method are simple and sensitive. The mechanism of the anions affections on the antioxidant activity of CeO_2 nanoparticles was also explored. These results not only add basic knowledge to the antioxidant activity of CeO_2 nanoparticles under different situations, but also pave the way for practical applications of nanoceria.

2. Experimental section

2.1. Materials and reagents

Poly (dimethyldiallylammonium chloride) (PDDA), double-stranded calf thymus DNA (ds-DNA), and tris(2,2'-bipyridyl)dichlororuthenium(II) hexahydrate ($Ru(bpy)_3Cl_2 \cdot 6H_2O$) were purchased from Sigma-Aldrich. Potassium chloride (KCl), potassium dihydrogen phosphate(KH_2PO_4), dipotassium hydrogen phosphate (K_2HPO_4), potassium sulfate (K_2SO_4), potassium hydrogen carbonate($KHCO_3$), hydrogen peroxide (H_2O_2, 30%), hexamethylenetetramine (HMT), and cerium (III) nitrate hexahydrate ($Ce(NO_3)_3 \cdot 6H_2O$) were purchased from Sinopharm Chemical Reagent Co., Ltd. (Beijing, China). All reagents were of analytical grade and were used without further purification. Millipore Milli Q (18 MΩ cm) water was used in all experiments.

2.2. Synthesis of the nanoparticles

Cerium oxide nanoparticles were prepared by reference to our previous report (Xue et al., 2011). First, HMT (0.125 M) was added to $Ce(NO_3)_3 \cdot 6H_2O$ solution (0.025 M) drop-wise with continuous stirring. Thereafter, the mixed aqueous solution was transferred into an autoclave (50 mL). Then, treat the solution at 100°C for 2 h in a hydrothermal way. After the solution was cooled to room temperature, cerium oxide powder was obtained by centrifuging. At last, cerium oxide powder was washed with water and ethanol followed by oven drying in vacuum.

The suspension of cerium oxide nanoparticles (10 μM) was obtained through dispersing them in deionized water, which needed to be sonicated prior to use.

2.3. Characterization of the nanoparticles

A transmission electron microscope (TEM) of FEI Tecnai G2 T20 was used to obtain the nanoparticles' morphology and size. Dynamic light scattering (DLS) was performed by Zetasizer potential/particle sizer NICOMP 380zls analyzer to measure the size distribution of the suspended CeO_2 particles. X-ray diffraction analysis (XRD) was measured by using a Bruker D8 Advance X-ray diffractometer. The corresponding operations and parameters were the same as those described in our previous study (Xue et al., 2011). The surface chemistry of the CNPs was studied by X-ray photoelectron spectroscopy (XPS) with an ESCALAB 250 Xi system. In this system, a base pressure of 1027 Torr and Al Ka X-ray radiation of 150 W was selected. The binding energies were referenced to the C 1s line at 284.8 eV from adventitious carbon.

2.4. The preparation of PDDA/DNA modified electrodes

SWV was measured using a CHI 440 electrochemical workstation (CH Instruments, China) with a three-electrode system. The system consists of a film-coated basal plane pyrolytic graphite (PG, geometric area 0.13 cm^2) disk as the working electrode, an Ag/AgCl (saturated KCl) electrode as the reference and a Pt wire as the counter electrode.

Prior to use, the PG working electrode was polished with 0.05 μm alumina powder and successively washed and sonicated with water, ethanol and water. Thereafter, a drop of positively charged PDDA solution (30 μL, 1 mg mL^{-1}, containing 0.1 M NaCl) was dropped onto the freshly polished electrode. After 20 min, the electrode was washed with water and dried with nitrogen stream. Subsequently, a drop of negatively charged DNA solution (30 μL, 1 mg mL^{-1}, in pH 7.0 PBS containing 0.1 M NaCl) was dropped on the surface of electrode for about 20 min. After washed and dried, the PDDA/DNA modified working electrode was obtained (Zhou and Rusling, 2001).

2.5. Square wave voltammetric (SWV) detection

Square wave voltammetry (SWV) is a form of linear potential sweep voltammetry, in which the current at a working electrode is measured while a regular square-wave potential was applied (Mirceski et al., 2007). SWV has been widely used in the study of DNA damage (Chen et al., 2006; Zhou and Rusling, 2001). In this work SWV was used to investigate the DNA protection by cerium oxide nanoparticles. SWV scans were measured in PBS (pH 7.0, 0.1 M) containing 0.1 M NaCl and 50 μM [Ru $(bpy)_3Cl_2$]. The parameters were as follows: frequency =15 Hz, amplitude=25 mV, and step=4 mV. Each SWV scan was repeated three times or more. All experiments were performed at 37 °C.

Firstly, the SWV scan of PDDA/DNA modified electrodes were obtained in the electrochemical cell containing PBS (pH 7.0, 10 mL) with 0.1 M NaCl and 50 μM ruthenium(II) tris(2,2'-bipyridyl) ($[Ru(bpy)_3]^{2+}$). Thereafter, the damage or protection processes were carried out. For DNA damage, the PDDA/DNA modified electrodes were incubated in injury solution with continuous stirring for 20 min. Then electrodes were washed with water and transferred to the electrochemical cell for SWV detection. The damage solution were obtained as follows: H_2O_2 (1 mL) was add into water or a series of solutions containing different anions (9 mL), and these mixtures were stabilized for 10 min prior to use. All experiments were performed at 37° C. For DNA protection, corresponding mixtures were replaced by adding a suspension of CeO_2 nanoparticles (50 μL, 10 μM) to the DNA damage solutions mentioned above before the addition of H_2O_2. Other experimental operations were the same as described in the section of DNA damage.

The simulated intracellular fluid contained 1 mM KCl, 10 mM K_2SO_4, 10 mM $KHCO_3$ and 50 mM K_2HPO_4/KH_2PO_4 (Jin et al., 2006). The intercellular fluid comprised of 114 mM KCl, 0.5 mM K_2SO_4, 30 mM $KHCO_3$ and 1 mM K_2HPO_4/KH_2PO_4 (Jin et al., 2006).

3. Results and discussion

3.1. Characterization of CeO_2 nanoparticles

The nanoparticles were synthesized by a hydrothermal method

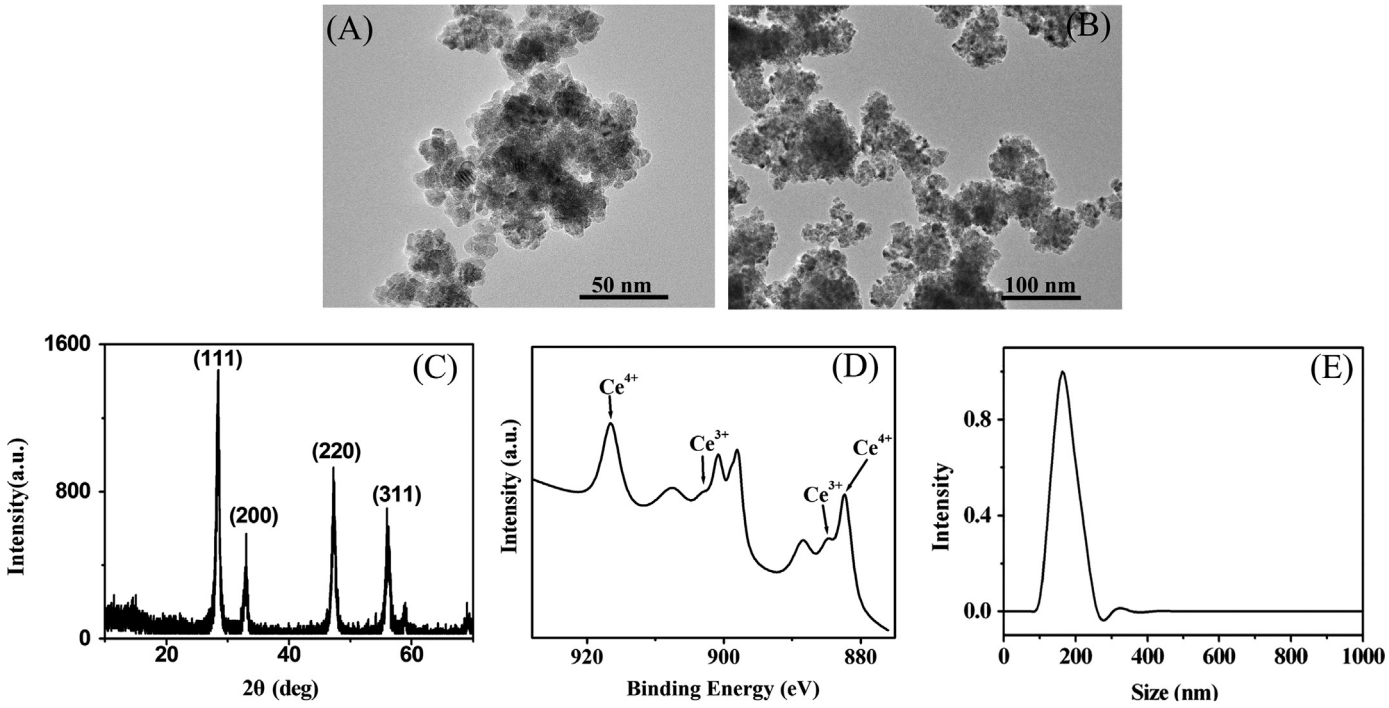

Fig. 1. Characterization of CeO_2 Nanoparticles. (A) TEM image. (B) TEM image of aggregation of CNPs. (C) XRD pattern. (D) XPS pattern. (E) DLS pattern.

(Tok et al., 2007). The XRD pattern indicated that cerium oxide formed due to the presence of the typical fluorite cubic structure (JCPDS card: 34-0394) (Fig. 1C). Additionally, binding energy peaks of both Ce^{3+} and Ce^{4+} were obtained from the XPS, suggesting the presence of mixed valence states (Ce^{3+} and Ce^{4+}) on the surface of synthesized nanoparticles (Fig. 1D), which also proved the successful synthesis of the nanoceria. The presence of the mixed valence state is vital to the antioxidant activity of CeO_2 nanoparticles, because the antioxidant activity is derived from the cycling between Ce^{3+} and Ce^{4+} on the surface of particles. Their morphology and size were examined by TEM and DLS. The TEM image shows that the size of the CeO_2 nanoparticles was in the range 5–10 nm (Fig. 1A) with a certain degree of aggregation, and TEM studies indicated the size of the aggregates was about 70–160 nm (Fig. 1B), while DLS indicated that the average size of aggregates was 170 nm (Fig. 1E), which proved further the aggregation of the CeO_2 nanoparticles. It has been proved that the aggregation in that degree has no effect on the antioxidant properties of the particles (Xue et al., 2011, 2012).

3.2. The electrochemical behavior of CeO_2 nanoparticles in multiple anions solutions

It is believed that antioxidant activity of CeO_2 nanoparticles was affected by external anions (Singh et al., 2011; Xue et al., 2012). As significant part of internal environment, four main anions exist in intracellular fluid and intercellular fluid. Moreover, the concentrations of these four anions varied considerably between intracellular fluid and intercellular fluid. Therefore, simulated intracellular fluid and intercellular fluid were prepared with different concentrations of anions, which were used for the study of the antioxidant activity of CeO_2 nanoparticles.

An electrochemical DNA biosensor was used to study the behavior of CeO_2 nanoparticles in simulated intracellular fluid and intercellular fluid in this work. The DNA biosensor was obtained by modifying ds-DNA on an electrode with a layer-by-layer assembly method, and then transferred to a solution of $[Ru(bpy)_3]^{2+}$ for SWV scan. $[Ru(bpy)_3]^{2+}$ could be recycled on an electrode with a catalytic current forming, as a result of being reduced from $[Ru(bpy)_3]^{3+}$ by guanine bases in DNA (Johnston et al., 1995; Thorp,

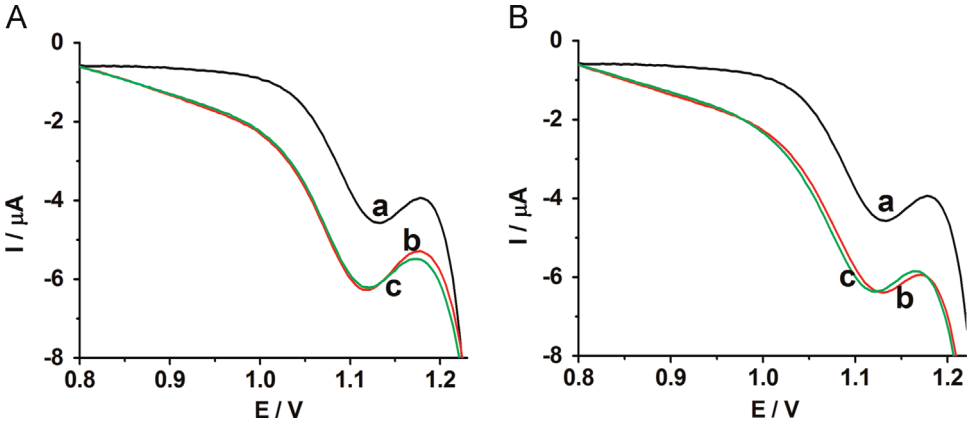

Fig. 2. SWV scans of PDDA/DNA films modified on a PG electrode in pH 7.0 PBS of $[Ru(bpy)_3]^{2+}$ (50 μM): incubated for 20 min in simulated intracellular fluid (A) or simulated intercellular fluid (B): (a) without other agents, (b) with H_2O_2, and (c) with CeO_2/H_2O_2.

1998). The more guanine bases accessible to $[Ru(bpy)_3]^{2+}$, the bigger the current enhanced (Rusling, 2004). In this system, H_2O_2 was used as hydroxyl radical ($\cdot OH$) generator, which could result in the damage of DNA double-helix structure. Then there should be more guanines were exposed, thus the electric current should increase. If CeO_2 could scavenge free radical, there would be less guanine exposed, and then the electro-current would decrease.

Fig. 2A shows the SWV behavior of PDDA/DNA modified electrode in pH 7.0 PBS of $[Ru(bpy)_3]^{2+}$ after incubated in simulated intracellular fluid at different conditions. An obvious peak could be observed in the curve a, which attributed to the electrocatalytic oxidation of $[Ru(bpy)_3]^{2+}$ by accessible guanine bases in DNA. After DNA was incubated in the simulated intracellular fluid solution, in which H_2O_2 was added beforehand, the SWV signal increased remarkably compared with the value of curve a (curve b). That means more guanines were exposed and available to $Ru(bpy)_3^{2+}$, resulting from the destruction of the double-helix structure of DNA. That is to say, the presence of multiple anions had no effect on the damage of DNA by H_2O_2. After the addition of CeO_2 nanoparticles the electrochemical signal is about the same with the absence of CeO_2 nanoparticles (curve c), suggesting CeO_2 nanoparticles did not protect DNA by scavenging free radical in simulated intracellular fluid solution. That is to say, the existence of multiple anions may affect the antioxidant activity of CeO_2 nanoparticles in simulated intracellular fluid. To further evaluate the effect of multiple anions on the antioxidant activity of CeO_2 nanoparticles, the behavior of CeO_2 was also studied in simulated intercellular fluid. Similarly, the addition of CeO_2 nanoparticles also did not bring an obvious decrease in the SWV signals (Fig. 2B), suggesting that CeO_2 nanoparticles could not protect DNA from damage by eliminating free radicals in simulated intercellular fluid, either. That is to say, multiple anions had an influence on the antioxidant activity of CeO_2 nanoparticles.

Then, the reason for the loss of antioxidant activity of CeO_2 nanoparticles in multiple anions was studied. The composition of the multiple anions solutions is relatively simple, HPO_4^{2-}, HCO_3^-, Cl^- and SO_4^{2-}. As was found, 0.1 M Cl^- or SO_4^{2-} did not affect the antioxidant activity of CeO_2 nanoparticles while 0.1 M PO_4^{3-} caused the loss of the antioxidant activity of CeO_2 nanoparticles in our previous study (Xue et al., 2012). Additionally, it was reported that a concentration of 0.1 mM or above PO_4^{3-} caused a shift in redox state of CeO_2 nanoparticles (Singh et al., 2011). However, the concentration of PO_4^{3-} is 1 mM in stimulated intercellular fluid, and reaches to 50 mM in stimulated intracellular fluid. Thus, we considered that maybe PO_4^{3-} with the physiological concentrations still had effect on the antioxidant activity of CeO_2 nanoparticles. Therefore, the antioxidant activity of CeO_2 nanoparticles was studied further in the multiple anions solutions without HPO_4^{2-} (Fig. 3). After DNA was treated with H_2O_2/simulated intracellular fluid or H_2O_2/simulated intercellular fluid without HPO_4^{2-}, the SWV peak current value became larger (curve b) than that of intact DNA (curve a) in both cases, suggesting DNA was also damaged in both cases. However, through comparing curves b with c, the addition of CeO_2 nanoparticles just resulted in a little decrease in the SWV signals in the both systems of multiple anions solutions without HPO_4^{2-}. Then it is concluded that except PO_4^{3-}, there should be other factors affecting the antioxidant activity of CeO_2 nanoparticles. As pointed out previously,

0.1 M Cl^- and SO_4^{2-} did not affect the antioxidant activity of CeO_2 nanoparticles (Xue et al., 2012). Moreover, in simulated intracellular fluid and simulated intercellular fluid, the higher concentration of Cl^- used was 114 mM, a little more than 0.1 M and the higher concentration of SO_4^{2-} used was 10 mM far lower than 0.1 M. Therefore, we speculated both Cl^- and SO_4^{2-} used in this work should have no effect on the antioxidant activity of CeO_2 nanoparticles. Thus, it considered that HCO_3^- may have a passive effect on the antioxidant activity of CeO_2 nanoparticles. To assure this, the antioxidant activity of CeO_2 nanoparticles was studied in the reaction mixtures solution only containing Cl^- and SO_4^{2-}. As shown in Fig. 4, when DNA was treated with H_2O_2/simulated intracellular fluid or H_2O_2/simulated intercellular fluid only containing Cl^- and SO_4^{2-}, the SWV peak current became larger (curve b) than that of intact DNA (curve a) in both cases, which indicates that the DNA was also damaged under these two reaction systems. However, the addition of CeO_2 nanoparticles led to obvious decreases in the SWV signal in both solutions by comparing curves b and c, which suggest that the CeO_2 nanoparticles could eliminate free radicals and reveal their protective effect on DNA in both simulated cellular fluid only containing Cl^- and SO_4^{2-}.

From the results above, it could be basically concluded that the existence of Cl^- and SO_4^{2-} did not affect the antioxidant activity of CeO_2 nanoparticles, while the existence of HCO_3^- also caused the loss of antioxidant activity of CeO_2 nanoparticles in the simulated cellular fluid. To clarify the effect of HCO_3^- and HPO_4^{2-} further, the antioxidant activity of CeO_2 nanoparticles was studied directly in the 1 mM PBS solution or 10 mM $KHCO_3$ solution (a lower concentration was selected between simulated intracellular fluid and simulated intercellular fluid), respectively. As show in Fig. 5, when DNA was treated with H_2O_2/1 mM PBS solution or H_2O_2/10 mM $KHCO_3$ solution, the SWV peak current became larger (curve b) than that of intact DNA (curve a) in both cases, which means that the DNA was also damaged in 1 mM PBS solution or 10 mM $KHCO_3$ solution. No obvious decreases of the SWV signal were found with the addition of CeO_2 nanoparticles in both

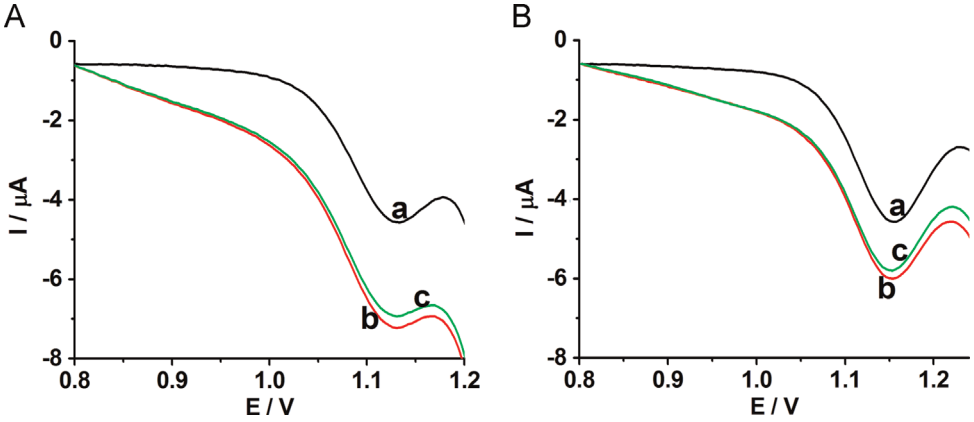

Fig. 3. SWV scans of PDDA/DNA films modified on a PG electrode in pH 7.0 PBS of $[Ru(bpy)_3]^{2+}$ (50 μM): incubated for 20 min in simulated intracellular fluid without HPO_4^{2-} (A) or simulated intercellular fluid without HPO_4^{2-} (B): (a) without other agents, (b) with H_2O_2, and (c) with CeO_2/H_2O_2.

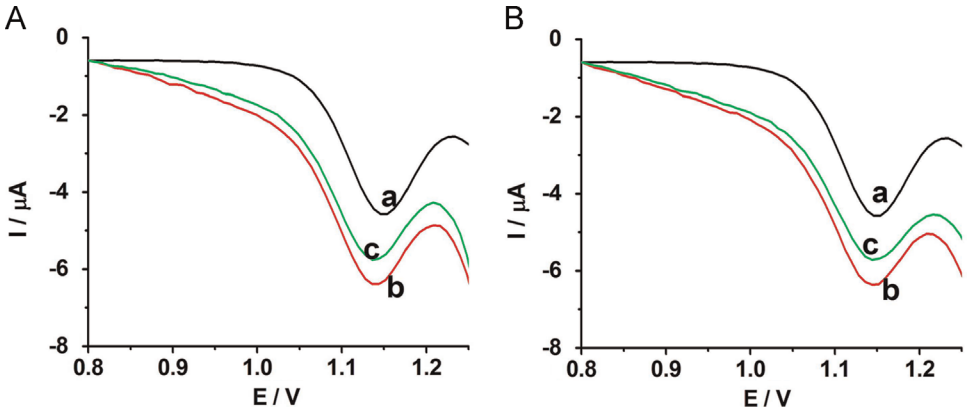

Fig. 4. SWV scans of PDDA/DNA films modified on a PG electrode in pH 7.0 PBS of $[Ru(bpy)_3]^{2+}$ (50 μM): incubated for 20 min in simulated intracellular fluid (A) or simulated intercellular fluid (B) only containing Cl^- and SO_4^{2-}: (a) without other agents, (b) with H_2O_2, and (c) with CeO_2/H_2O_2.

solutions by comparing curves b and c, which suggested CeO_2 nanoparticles had no protection effect on DNA damage in 1 mM PBS solution (Fig. 5A) or 10 mM $KHCO_3$ solution (Fig. 5B). Up to now, it is clear that both HPO_4^{2-} and HCO_3^- affected the antioxidant activity of CeO_2 nanoparticles in the simulated intracellular fluid and simulated intercellular fluid. To show more clearly, all the results have been given in the form of bar diagrams with error bars in the supplementary file (Figs. S1–S4).

3.3. *Mechanism of different anions' affection on antioxidant activity of CeO_2 nanoparticles*

From the results above, it was found that main anions in intracellular fluid and intercellular fluid had different effects on the antioxidant activity of CeO_2 nanoparticles. Cl^- or SO_4^{2-} have no affected the antioxidant activity of CeO_2 nanoparticles while HPO_4^{2-} and HCO_3^- made CeO_2 nanoparticles lose its antioxidant activity. As well know, the antioxidant activity of CeO_2 nanoparticles is derived from the redox cycling between Ce^{3+} and Ce^{4+} on the surface of CeO_2 nanoparticles (Chen et al., 2006; Das et al., 2007; Hirst et al., 2009; Tsunekawa et al., 1999). Meantime, it was surmised that specific anions may interrupt the redox cycling by interacting with cerium ion on the surface of CeO_2 nanoparticles (Singh et al., 2011; Xue et al., 2012), resulting the loss of antioxidant activity of CeO_2 nanoparticles. In this work, maybe the redox cycling was broken by phosphate group and carbonate group interacting with cerium ion on the surface of CeO_2 nanoparticles. To make it clear, the CeO_2 nanoparticles treated with simulated intracellular fluid or intercellular fluid was analyzed by XPS, respectively. Prior to use, the CeO_2 nanoparticles was washed adequately to avoid the simple adsorption of anions on the nanoparticles' surface. However, in spectrum of CeO_2 treated with simulated intracellular fluid, an obvious binding energy peak appeared at 132.7 eV which was absent in the spectrum of CeO_2 without treated. The binding energy peak should be assigned to "P" 2p core level (Pelavin et al., 1970). Moreover, compared with the binding energy peak value of 132.1 eV of "P" 2p core level spectrum of phosphate buffer (Fig. 6C, upper), 0.6 eV shift toward higher binding energy, which should be assigned to the interaction of PO_4^{3-} with cerium ions on the surface of CeO_2 nanoparticles (Singh et al., 2011). Therefore, it is suggested the whole mechanism was probably as follows in this work: in both simulated intracellular fluid and simulated intercellular fluid only containing Cl^- and SO_4^{2-}, the redox cycle between Ce^{3+} and Ce^{4+} on the surface of CeO_2 nanoparticles went on well. Ce^{3+} ions were converted into Ce^{4+} by reacting with free radical, and then Ce^{3+} ions were regenerated for reduction of Ce^{4+} on the surface of the nanoparticles (Perez et al., 2008; Xue et al., 2012). Thus, CeO_2 nanoparticles can eliminate the free radicals continually and show good antioxidant activity. However, when encountering with phosphate group, cerium ions on the surface of CeO_2 nanoparticles would form cerium phosphate, and the formantion of cerium phosphate would interrupt the redox cycling between Ce^{3+} and Ce^{4+}(Singh et al., 2011; Xue et al., 2012). As a result, CeO_2 nanoparticles lose the ability of scavenging free radicals, and could not protect DNA from oxidation any more in the solutions containing HPO_4^{2-}.

Meantime, an obvious binding energy peak appeared at 288.7 eV in spectrum of CeO_2 treated with simulated intracellular fluid (Fig. 6D, down). It should be assigned to the characteristic

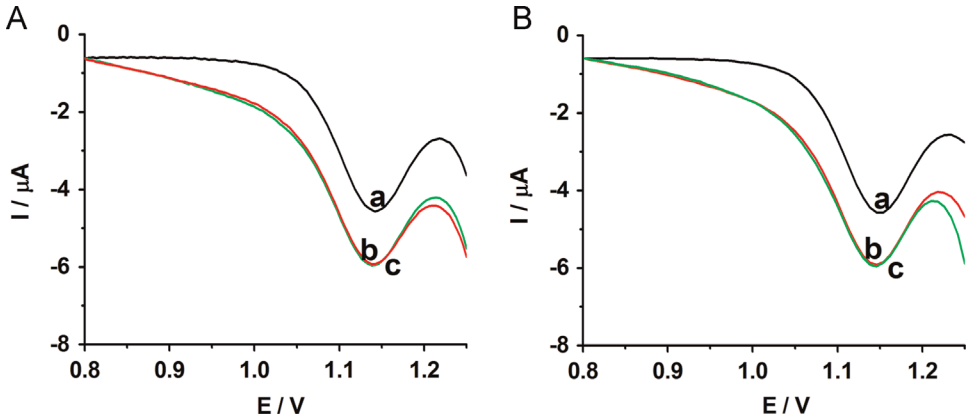

Fig. 5. SWV scans of PDDA/DNA films modified on a PG electrode in pH 7.0 PBS of $[Ru(bpy)_3]^{2+}$ (50 μM): incubated for 20 min in 1 mM PBS solution (A) or 10 mM $KHCO_3$ solution (B): (a) without other agents, (b) with H_2O_2, and (c) with CeO_2/H_2O_2.

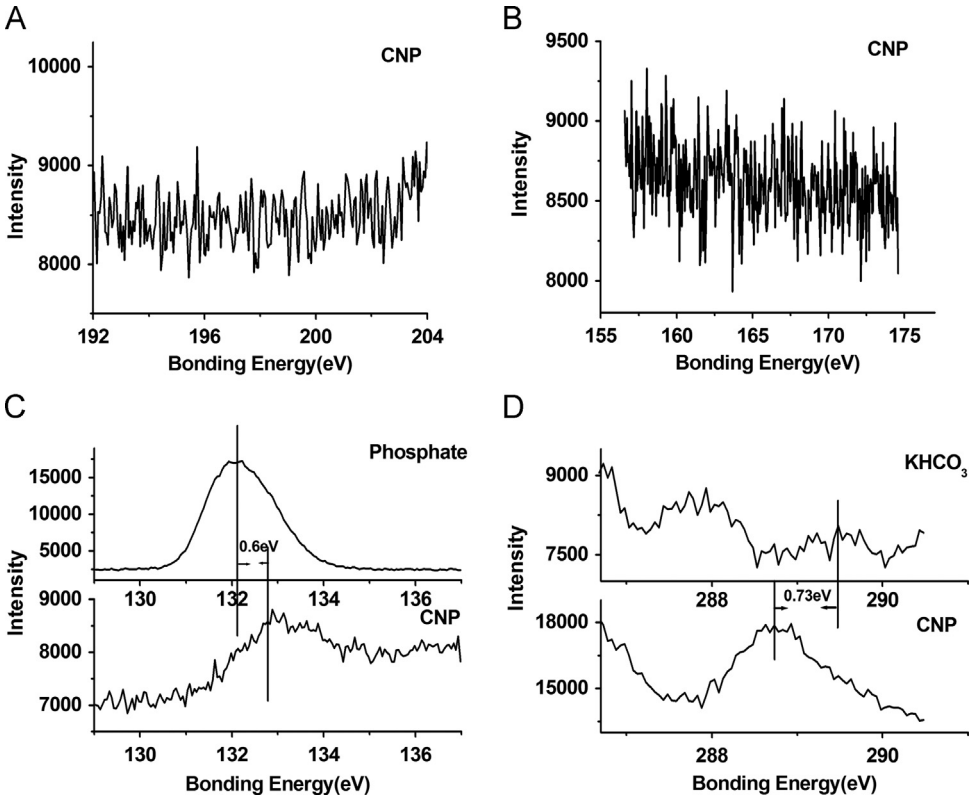

Fig. 6. Different parts of XPS spectra of CeO_2 nanoparticles treated with simulated intracellular fluid, which belong to the range of binding energy peak of Cl element (A), S element (B), P element (C), C element (D).

absorption peak of C in carbonate. In addition, 0.73 eV shift toward lower binding energy compared to C spectra obtained from potassium bicarbonate alone (Fig. 6) (Gelius et al., 1971), suggesting that there is also interaction between carbonate and cerium ions on the surface of CeO_2 nanoparticles. Hence, it is think that carbonate group affected the antioxidant activity of CeO_2 nanoparticles as same as phosphate group.

Additionally, it should be noted that, no obvious peak was found from 192 eV to 204 eV (Tsubouchi et al., 2013), indicating that there was no chlorine element on the surface of CeO_2 nanoparticles (Fig. 6A). Similarly, we did not find obvious peak in the range of 157–175 eV (Fig. 6B), suggesting that no sulfur element existed on the surface of CeO_2 nanoparticles, either (Fantauzzi et al., 2014). These results suggest that Cl^- and SO_4^{2-} did not interact with cerium ions on the surface of CeO_2 nanoparticles as phosphate group and carbonate group did. Therefore, the redox cycling between Ce^{3+} and Ce^{4+} took place unhindered on the surface of CeO_2 nanoparticles. It should be the reason why CeO_2 nanoparticles revealed good antioxidant activity in the multiple anions solutions only containing Cl^- and SO_4^{2-}. The same phenomena were found in the spectrum of CeO_2 treated with simulated intercellular fluid (Fig. S5), which verified the result further.

4. Conclusion

In this work, the antioxidant activity of CeO_2 nanoparticles was evaluated in simulated intracellular fluid or simulated intercellular fluid with an electrochemical DNA biosensor. The presence of HPO_4^{2-} and HCO_3^- caused the loss of antioxidant activity of CeO_2 nanoparticles in both systems by forming the cerium salt on the surface of nanoparticles. These results not only add basic knowledge to the antioxidant activity of CeO_2 nanoparticles under different situations, but also pave the way for practical applications of nanoceria. However, it is worth noting that CeO_2 nanoparticles revealed antioxidant activity in many kinds of cells (Chen et al., 2006; Colon et al., 2009; D'Angelo et al., 2009; Das et al., 2007; Karakoti et al., 2009; Perez et al., 2008; Schubert et al., 2006; Tarnuzzer et al., 2005; Xia et al., 2008), in which HPO_4^{2-} and HCO_3^- group must exist. Therefore, it need more study to clarify the paradoxical phenomena for a better use of antioxidant activity of CeO_2 nanoparticles. Then electrochemical DNA biosensor is an effective method to explore the antioxidant activity of CeO_2 nanoparticles, which would also widen the application scope of this DNA electrochemical biosensor.

Acknowledgements

This work was supported by the National Natural Science Foundation of China (21271184) and the Ministry of Science and Technology of China (973 program 2014CB931900 and 2012CB932504).

Appendix A. Supplementary Information

Supplementary data associated with this article can be found in the online version at http://dx.doi.org/10.1016/j.bios.2015.03.030.

References

Aalapati, S., Ganapathy, S., Manapuram, S., Anumolu, G., Prakya, B.M., 2014. Toxicity and bio-accumulation of inhaled cerium oxide nanoparticles in CD1 mice. Nanotoxicology 8 (7), 786–798.

Arya, A., Sethy, N.K., Singh, S.K., Das, M., Bhargava, K., 2013. Cerium oxide nanoparticles protect rodent lungs from hypobaric hypoxia-induced oxidative stress and inflammation. Int. J. Nanomed. 8, 4507–4519.

Auffan, M., Rose, J., Orsiere, T., De Meo, M., Thill, A., Zeyons, O., Proux, O., Masion, A., Chaurand, P., Spalla, O., Botta, A., Wiesner, M.R., Bottero, J.Y., 2009. CeO_2 nanoparticles induce DNA damage towards human dermal fibroblasts in vitro. Nanotoxicology 3 (2) 161-U115.

Bakht, M.K., Hosseini, V., Honarpisheh, H., 2013. Radio labeled nanoceria probes may reduce oxidative damages and risk of cancer: A hypothesis for radioisotope-based imaging procedures. Med. Hypotheses 81 (6), 1164–1168.

Celardo, I., Pedersen, J.Z., Traversa, E., Ghibelli, L., 2011. Pharmacological potential of cerium oxide nanoparticles. Nanoscale 3 (4), 1411–1420.

Chen, J.P., Patil, S., Seal, S., McGinnis, J.F., 2006. Rare earth nanoparticles prevent retinal degeneration induced by intracellular peroxides. Nat. Nanotechnol. 1 (2), 142–150.

Colon, J., Herrera, L., Smith, J., Patil, S., Komanski, C., Kupelian, P., Seal, S., Jenkins, D. W., Baker, C.H., 2009. Protection from radiation-induced pneumonitis using cerium oxide nanoparticles. Nanomed.-Nanotechnol. 5 (2), 225–231.

D'Angelo, B., Santucci, S., Benedetti, E., Di Loreto, S., Phani, R.A., Falone, S., Amicarelli, F., Ceru, M.P., Cimini, A., 2009. Cerium oxide nanoparticles trigger neuronal survival in a human Alzheimer disease model by modulating BDNF pathway. Curr. Nanosci. 5 (2), 167–176.

Das, M., Patil, S., Bhargava, N., Kang, J.F., Riedel, L.M., Seal, S., Hickman, J.J., 2007. Auto-catalytic ceria nanoparticles offer neuroprotection to adult rat spinal cord neurons. Biomaterials 28 (10), 1918–1925.

Fantauzzi, M., Rigoldi, A., Elsener, B., Atzei, D., Rossi, A., 2014. A contribution to the surface characterization of alkali metal sulfates. J. Electron Spectrosc. 193, 6–15.

Gelius, U., Allan, C.J., Johansson, lG., Siegbahn, H., Allison, D.A., Siegbahn, K., 1971. The ESCA spectra of benzene and the iso-electronic series, thiophene, pyrrole and furan. Phys. Scr. 3, 237–242.

Heckman, K.L., DeCoteau, W., Estevez, A., Reed, K.J., Costanzo, W., Sanford, D., Leiter, J.C., Clauss, J., Knapp, K., Gomez, C., Mullen, P., Rathbun, E., Prime, K., Marini, J., Patchefsky, J., Patchefsky, A.S., Hailstone, R.K., Erlichman, J.S., 2013. Custom cerium oxide nanoparticles protect against a free radical mediated autoimmune degenerative disease in the brain. ACS Nano 7 (12), 10582–10596.

Hirst, S.M., Karakoti, A.S., Tyler, R.D., Sriranganathan, N., Seal, S., Reilly, C.M., 2009. Anti-inflammatory properties of cerium oxide nanoparticles. Small 5 (24), 2848–2856.

Jin, G.Q., Li, Z., Hou, J.M., Ren, Y., 2006. Biochemistry. Shanghai Scientific and Technical Publishers (SSTP).

Johnston, D.H., Glasgow, K.C., Thorp, H.H., 1995. Electrochemical measurement of the solvent accessibility of nucleobases using electron-transfer between DNA and metal-complexes. J. Am. Chem. Soc. 117 (35), 8933–8938.

Karakoti, A., Singh, S., Dowding, J.M., Seal, S., Self, W.T., 2010. Redox-active radical scavenging nanomaterials. Chem. Soc. Rev. 39 (11), 4422–4432.

Karakoti, A.S., Singh, S., Kumar, A., Malinska, M., Kuchibhatla, S.V.N.T., Wozniak, K., Self, W.T., Seal, S., 2009. PEGylated nanoceria as radical scavenger with tunable redox chemistry. J. Am. Chem. Soc. 131 (40), 14144–14145.

Korsvik, C., Patil, S., Seal, S., Self, W.T., 2007. Superoxide dismutase mimetic properties exhibited by vacancy engineered ceria nanoparticles. Chem. Commun. 10, 1056–1058.

Lee, S.S., Song, W., Cho, M., Puppala, H.L., Nguyen, P., Zhu, H., Segatori, L., Colvin, V. L., 2013. Antioxidant properties of cerium oxide nanocrystals as a function of nanocrystal diameter and surface coating. ACS Nano 7 (11), 9693–9703.

McGinnis, J.F., Stepanik, P.L., Chen, W., Elias, R., Cao, W., Lerious, V., 1999. Unique retina cell phenotypes revealed by immunological analysis of recoverin expression in rat retina cells. J. Neurosci. Res. 55, 252–260.

Mirceski, V., Komorsky-Lovric, Š., Lovric, M., 2007. Square-wave Voltammetry: Theory and Application. Springer-Verlag, Berlin.

Niu, J.L., Azfer, A., Rogers, L.M., Wang, X.H., Kolattukudy, P.E., 2007. Cardioprotective effects of cerium oxide nanoparticles in a transgenic murine model of cardiomyopathy. Cardiovasc. Res. 73 (3), 549–559.

Pagliari, F., Mandoli, C., Forte, G., Magnani, E., Pagliari, S., Nardone, G., Licoccia, S., Minieri, M., Di Nardo, P., Traversa, E., 2012. Cerium oxide nanoparticles protect cardiac progenitor cells from oxidative stress. ACS Nano 6 (5), 3767–3775.

Park, E.J., Choi, J., Park, Y.K., Park, K., 2008. Oxidative stress induced by cerium oxide nanoparticles in cultured BEAS-2B cells. Toxicology 245 (1–2), 90–100.

Pelavin, M., Hendbrickson, D.N., Hollander, J.M., Jolly, W.L., 1970. Phosphorus 2p electron binding energies correlation with extended Huckel charges. J. Phys. Chem. 74, 1116–1121.

Perez, J.M., Asati, A., Nath, S., Kaittanis, C., 2008. Synthesis of biocompatible dextran-coated nanoceria with pH-dependent antioxidant properties. Small 4 (5), 552–556.

Rich, T., Allen, R.L., Wyllie, A.H., 2000. Defying death after DNA damage. Nature 407 (6805), 777–783.

Rusling, J.F., 2004. Sensors for toxicity of chemicals and oxidative stress based on electrochemical catalytic DNA oxidation. Biosens. Bioelectron. 20 (5), 1022–1028.

Schubert, D., Dargusch, R., Raitano, J., Chan, S.W., 2006. Cerium and yttrium oxide nanoparticles are neuroprotective. Biochem. Biophys. Res. Commun. 342 (1), 86–91.

Singh, S., Dosani, T., Karakoti, A.S., Kumar, A., Seal, S., Self, W.T., 2011. A phosphate-dependent shift in redox state of cerium oxide nanoparticles and its effects on catalytic properties. Biomaterials 32 (28), 6745–6753.

Tarnuzzer, R.W., Colon, J., Patil, S., Seal, S., 2005. Vacancy engineered ceria nanostructures for protection from radiation-induced cellular damage. Nano Lett. 5 (12), 2573–2577.

Thorp, H.H., 1998. Cutting out the middleman: DNA biosensors based on electrochemical oxidation. Trends Biotechnol. 16 (3), 117–121.

Tok, A.I.Y., Du, S.W., Boey, F.Y.C., Chong, W.K., 2007. Hydrothermal synthesis and characterization of rare earth doped ceria nanoparticles. Mater. Sci. Eng. A 466 (1–2), 223–229.

Tsai, Y.Y., Oca-Cossio, J., Agering, K., Simpson, N.E., Atkinson, M.A., Wasserfall, C.H., Constantinidis, I., Sigmund, W., 2007. Novel synthesis of cerium oxide nanoparticles for free radical scavenging. Nanomedicine 2 (3), 325–332.

Tsubouchi, N., Saito, T., Ohtaka, N., Nakazato, Y., Ohtsuka, Y., 2013. Chlorine release during fixed-bed gasification of coal chars with carbon dioxide. Energy Fuel 27 (9), 5076–5082.

Tsunekawa, S., Sivamohan, R., Ohsuna, T., Kasuya, A., Takahashi, H., Tohji, K., 1999. Ultraviolet absorption spectra of CeO2 nano-particles In: Woodward, R.C. (Ed.), Rare Earths"98. Transtec Publications Ltd., Zurich-Uetikon, pp. 439–445.

Xia, T., Kovochich, M., Liong, M., Madler, L., Gilbert, B., Shi, H.B., Yeh, J.I., Zink, J.I., Nel, A.E., 2008. Comparison of the mechanism of toxicity of zinc oxide and cerium oxide nanoparticles based on dissolution and oxidative stress properties. ACS Nano 2 (10), 2121–2134.

Xue, Y., Luan, Q.F., Yang, D., Yao, X., Zhou, K.B., 2011. Direct evidence for hydroxyl radical scavenging activity of cerium oxide nanoparticles. J. Phys. Chem. C 115 (11), 4433–4438.

Xue, Y., Zhai, Y.W., Zhou, K.B., Wang, L., Tan, H.N., Luan, Q.F., Yao, X., 2012. The vital role of buffer anions in the antioxidant activity of CeO_2 nanoparticles. Chem.-Eur. J. 18 (35), 11115–11122.

Yu, L., Lu, Y., Man, N., Yu, S.H., Wen, L.P., 2009. Rare earth oxide nanocrystals induce autophagy in HeLa cells. Small 5 (24), 2784–2787.

Zhang, Y., Zhou, K.B., Zhai, Y.W., Fei, Q., Pan, L.L., Yao, X., 2014. Crystal plane effects of nano-CeO_2 on its antioxidant activity. RSC Adv. 4, 50325–50330.

Zhou, L.P., Rusling, J.F., 2001. Detection of chemically induced DNA damage in layered films by catalytic square wave voltammetry using $Ru(Bpy)_3^{2}$. Anal. Chem. 73 (20), 4780–4786.